Available online at www.sciencedirect.com
SCIENCE DIRECT®
Electrochimica Acta 49 (2004) 1045–1055
ELECTROCHIMICA Acta
www.elsevier.com/locate/electacta

Nano-stuctured Pt–Fe/C as cathode catalyst in direct methanol fuel cell

Wenzhen Li [a,1], Weijiang Zhou [a], Huanqiao Li [a], Zhenhua Zhou [a], Bing Zhou [b], Gongquan Sun [a], Qin Xin [a,c,*]

[a] *Direct Alcohol Fuel Cell Laboratory, Dalian Institute of Chemical Physics, Chinese Academy of Sciences, Dalian 116023, China*
[b] *Headwaters Nano Kinetix, 1501 New York Avenue, Lawrenceville, NJ 08648, USA*
[c] *State Key Laboratory of Catalysis, Dalian Institute of Chemical Physics, Chinese Academy of Sciences, Dalian 116023, China*

Received 18 April 2003; received in revised form 27 October 2003; accepted 28 October 2003

Abstract

Pt–Fe/C catalysts were prepared by a modified polyol synthesis method in an ethylene glycol (EG) solution, and then were heat-treated under H_2/Ar (10 vol.%) at moderate temperature (300 °C, Pt–Fe/C300) or high temperature (900 °C, Pt–Fe/C900). As comparison, Pt–Fe/C alloy catalyst was prepared by a two-step method (Pt–Fe/C900B). X-ray diffraction (XRD) and transmission electron microscopy (TEM) images show that particles size of the catalyst increases with the increase of treatment temperatures. Pt–Fe/C300 catalyst has a mean particle size of 2.8 nm (XRD), 3.6 nm (TEM) and some Pt–Fe alloy was partly formed in this sample. Pt–Fe/C900B catalyst has the biggest particle size of 6.2 nm (XRD) and the best Pt–Fe alloy form. Cyclicvoltammetry (CV) shows that Pt–Fe/C300 has larger electrochemical surface area than other Pt–Fe/C and the highest utilization ratio of 76% among these Pt-based catalysts. Rotating disk electrode (RDE) cathodic curves show that Pt–Fe/C300 has the highest oxygen reduction reaction (ORR) mass activity (MA) and specific activity (SA), as compared with Pt/C catalyst in 1.0 M $HClO_4$. However, Pt–Fe/C catalyst does not appears to be a more active catalyst than Pt/C for ORR in 1.0 M $HClO_4$ + 0.1 M CH_3OH. Pt–Fe/C300 exhibits higher ORR activity and better performance than other Pt–Fe/C or Pt/C catalysts when employed for cathode in direct methanol single cell test, the enhancement of the cell performance is logically attributed to its higher ORR activity, which is probably attributed to more Pt^0 species existing and Fe ion corrosion from the catalyst.

Keywords: Platinum–iron alloy; Electrocatalyst; Cathode; Oxygen reduction reaction (ORR); Direct methanol fuel cell

1. Introduction

Direct methanol fuel cells (DMFCs) are attracting much more attention for their potentiality as clean and mobile power sources in the future [1–5]. At present, there are still two challenging research objectives in the fundamental research field in order to commercialize DMFCs in the transport power sources market. The first is to discover novel polymer electrolyte membranes, which has high proton conductivity and low methanol cross-over capability, and the second is to find novel anode catalyst, which can efficiently improve the electrode-kinetics of methanol oxidation, and to prepare cathode catalyst with high activity. Generally, the over-potential at the cathode in Polymer electrolyte fuel cells (PEFCs) is about 0.2 V because of the highly irreversible reaction oxygen reduction reaction (ORR), the situation is even worse in the DMFCs, for the methanol crossed over from anode poisoning cathode, which results in the severe potential loss of ca. 0.1 V even under open-circuit conditions [4]. This means a loss of about 25% from theoretical maximum efficiency only in cathode of a DMFC [6]. The present research on cathode catalysts are mainly two orientations, one is to find some methanol tolerant catalyst, such as metal phthalocynines, porphyrins, metal oxides, metal carbides and ruthenium-based chalcogenides, all which has certain ORR activity and methanol tolerant capability, but the life-time still need to improve [7–9]. The other is to use alloy catalysts of Pt with various transitional metals in order to improve ORR activity, carbon-supported binary and ternary-alloys of platinum, namely, Pt–Co/C, Pt–Cr/C, Pt–Ni/C, Pt–Fe/C and Pt–Cr–Co/C have been proved to offer good ORR performance in PAFCs, PEFCs and more recently in DMFCs [10–14]. The dispersion and the compositional homogeneity of the alloy clusters are important factors to obtain a good

* Corresponding author. Tel.: +86-411-4379071; fax: +86-411-4379071.
E-mail addresses: wenzhli@dicp.ac.cn (W. Li), xinqin@dicp.ac.cn (Q. Xin).
[1] Tel.: +86-411-4676788; fax: +86-411-4676788.

0013-4686/$ – see front matter © 2003 Elsevier Ltd. All rights reserved.
doi:10.1016/j.electacta.2003.10.015

electrocatalytic activity [10,15–17]. These Pt–M/C catalysts are prepared or/and treated at high temperature under inert or reducing atmosphere in order to form Pt–M alloy, this thermal treatment at high temperatures give rise to an undesired metal particle growth, by sintering of platinum particles (>5 nm) [7], therefore reduces the specific surface area of Pt–M/C catalyst and decreases the enhancement of activity of ORR for Pt–M/C catalyst.

Polyol synthesis method is a very efficient way to prepare noble metals or noble metal/transitional bimetallic clusters in nano-size [18–20], unsupported noble metal (Pt, Ru, Rh, etc.) nanoclusters with very small particle size and very narrow particle distribution were prepared according to the synthesis strategy [18]. Zhou et al. extended this synthesis strategy and prepared uniform carbon supported platinum nanoparticles with an average diameter of ca. 2.9 nm, the Pt metal loading was up to 40 wt.%, and the Pt/C catalyst showed enhanced ORR activity as comparing with commercial Pt/C (40 wt.% Johnson Matthey Corp.) in DMFC test [21]. Carbon supported Pt–Ru, Pt–Pd, Pt–W and Pt–Sn binary electrocatalysts with sharp particle size distribution were prepared via this modified polyol synthesis method and their ethanol oxidation activities were investigated [22]. Li et al. also prepared multi-walled carbon nanotubes (MWNTs) supported Pt catalyst via this modified polyol synthesis method and the Pt/MWNTs shows enhanced ORR activity as compared with Pt/C catalyst in DMFC tests [23,24].

In this paper, we used this modified polyol synthesis method to prepare a Pt–Fe/C catalyst, which was then reduced at moderated temperature (300 °C) under hydrogen atmosphere, thus avoiding being reduced at high temperature. As comparison, high temperature reduced in-house Pt–Fe/C sample Pt–Fe/C900 and Pt–Fe/C900B (using two-step precipitation method) were also prepared. Powder X-ray diffraction (XRD) characterization was carried out to determine the mean crystalline size and the Pt–Fe alloy effect of these Pt–Fe/C catalysts. Transmission electron microscopy (TEM) were used to investigate mean particle size and particle size distribution of catalysts. Electrochemical experiments including cyclicvoltammetry (CV), and rotating disk electrolyte (RDE), were also conducted to characterize these Pt–Fe/C catalysts, to determine the electrochemical area of the catalysts and to test the ORR activity of the catalysts with or without methanol effluence, respectively. These Pt based catalysts were employed as cathode catalysts in DMFC to investigate their ORR activity and single cell performance.

2. Experimental

2.1. Catalyst preparation

The support is carbon black Vulcan XC-72 (Carbot Corp., BET: 237 m^2/g, denoted as C) treated by 2 N HCl and 5 N HNO_3, following a procedure reported in ref. [25]. Pt–Fe/C catalyst was prepared by a modified polyol method (EG method) developed in our lab [21–24]. The detailed preparation process can be described as follow: hexachloroplatinic (IV) acid (H_2PtCl_6) and iron chloride ($FeCl_3$) solution were mixed well and added to carbon ethylene glycol solution (Pt metal loading: 20 wt.%, Pt:Fe = 3:1 in atomic ratio) under mechanically stirred conditions, hexachloroplatinic (IV) acid (H_2PtCl_6)and iron chloride ($FeCl_3$) solution were mixed well and added to carbon ethylene glycol solution (Pt metal loading: 20 wt.%, Pt:Fe = 3:1 in atomic ratio) under mechanically stirred conditions, 1.0 M NaOH (in EG solution) was added to adjust the pH of the solution to about 11, the temperature was increased to 130 °C for 3 h. The whole preparation process was conducted under a flowing argon (99 vol.%). After filtration, washing and drying procedures, the as-received Pt–Fe/C catalyst (Pt–Fe/C) was obtained. The Pt–Fe/C300 catalyst and Pt–Fe/C900 was obtained by heat-treating Pt–Fe/C at 300 or 900 °C under H_2/Ar (10 vol.% H_2) atmosphere for 2 and 1 h, respectively. Pt/C (prepared by EG method) and Pt/C300 catalysts (Pt/C was reduced at 300 °C under H_2/Ar) were used as reference samples. In order to examine Pt–Fe alloy effect, Pt–Fe/C900B (Pt:Fe = 3:1 in atomic ratio) was also prepared by a two-step method, namely, Fe deposits on Pt/C (prepared by EG method) according to a wet-incipience technique as ref. [11], then the Pt–Fe/C catalyst was heat-treated at 900 °C for 1 h under H_2/Ar.

2.2. Characterization

All the Pt-based catalysts were characterized by recording their powder X-ray diffraction (XRD) patterns on a Rigaku Rotalflex (RU-200B) X-ray diffractometer using Cu Kα radiation with a Ni filter. The tube current is 100 mA and tube voltage is 40 kV. The 2θ angular regions between 20 and 85° were explored at a scan rate of 7°/min and the 64–72° angular was scanned at 1°/min in order to obtain Pt particle size precisely using the Scherrer formula. The angular resolution in all the 2θ-scans was 0.02° for all XRD tests. TEM investigations were carried out in a JEOL JEM-2000EX operating at 100 kV to get information of the mean particle size and size distribution of Pt particles of the catalysts. The histogram of prepared Pt-based catalyst was made by measuring more than 300 particles. These Pt–Fe/C samples were subjected to energy dispersive analysis by X-rays (EDX) by employing JEOL JSM-5600LV scanning electron microscope with operating voltage of 20 kV to determine the composition of the elements in the catalysts.

Electrochemical characterization was performed on an EG&G 273A instrument, A conventional three-compartment electrochemical cell, in which reference counter and working electrodes were separated, was used for CV and RDE experiments, in which a SCE was used for the reference electrode and a platinum screen was used for the counter electrode. The catalyst layer on the RDE was prepared as follows: a mixture containing 5.0 mg Pt/C or Pt–Fe/C catalysts,

1.0 ml ethanol and 50.0 μl Nafion (5 wt.%) were ultrasonically blended in a glass vessel for half an hour to obtain a homogeneous ink. A 25 μl paint ink was spread on the surface of a glassy carbon electrode (area: 0.1256 cm^2) using a conventional method-micropipette and dried under 80 °C for 10 min to obtain a thin active catalytic layer. The electrolyte is 1.0 M $HClO_4$ solution, which were both obtained from high-purity perchloric acid (MOS grade) and two-distilled water. CV was obtained after high purity nitrogen clean the electrolyte solution for 20 min. The scan rate was 50 mV/s and scan range was from −0.2 to 1.2 V (SCE). RDE tests were obtained after oxygen bubbling for 10 min. The scan range was from 0.9 V to 0 V (SCE) at a rotating speed of 2500 rpm and the scan rate was 5 mV/s. Fe powder (99.99%) was diluted in $HClO_4$ solution in order to test Fe ion effect on activity of ORR on Pt/C catalyst. The net kinetic current of ORR was obtained by using the following formula:

$$i_{kin} = \frac{i_{lim} \cdot i_{obv}}{i_{lim} - i_{obv}} \quad (1)$$

where i_{kin} is the current derived from diffusion coupled kinetics in the porous reaction layer, i_{lim} is the limited current, i_{obv} is the obvious current. The mass activity (MA) for these Pt–Fe/C catalysts was the corresponding i_{kin} at the potential of 660 mV (SCE = 0.9 V·RHE), and the mass of Pt was calculated based on the 25 ul ink corresponding to a 0.119 mg Pt/C or 0.0238 mg Pt. The corresponding specific activity (SA) was obtained by the following formula:

$$SA = \frac{MA}{S_{ECSA}} \quad (2)$$

where S_{ECSA} is electrochemical surface area obtained from hydrogen desorption peaks in CV [26]. Both CV and RDE tests were carried out at room temperature.

2.3. Single cell test

The electrochemical activity of these Pt-based cathodic catalysts (metal loading: 1.0 mg/cm^2) in DMFC was examined. The anode catalysts were identically Pt–Ru/C (Johnson Matthey, 20 wt.% Pt, 10 wt.% Ru, 2.0 mg/cm^2 metal loading) and Nafion-115® (DuPont) were used as the membranes, the preparation of electrode was as the following procedure [27]. Both anode and cathode consist of a backing layer, a gas diffusion layer and a catalyst layer. Teflonized (30 wt.% Teflon in cathode, 10 wt.% Teflon in anode) carbon papers (SGL Corp., 270 μm in thickness) were employed as backing layers in these electrodes, 30 wt.% (or 10 wt.%) Teflon in carbon black XC-72 was suspended in ethanol and agitated in an ultrasonic water bath, then the slurry was spread to the carbon paper as gas diffusion layers. The diffusion layers for cathode and anode were about 30 μm The required amount of catalyst (Pt–Ru/C in anode, Johnson Matthey, 20 wt.% Pt, 10 wt.% Ru, 2.0 mg/cm^2 metal loading; in-house Pt-based catalyst (Pt/C or Pt–Fe/C sample) in cathode, 20 wt.%, 1.0 mg/cm^2) was mixed with 10 wt.% Nafion® (5 wt.% Nafion® solution) and brushed on the diffusion layers to constitute catalyst layers (ca. 50 μm in thickness). Finally, a thin layer of 5 wt.% Nafion® solution was spread on to the surface of each electrode (1.0 mg Nafion®/cm^2). Membrane electrode assembly (MEA) was obtained by pressing the cathode and anode on either side of a pretreated Nafion-115® membrane by compaction with a pressure of 50 kg/cm^2, at 135 °C for 3 min.

The DMFC was assembled by mounting the MEA into single cell with an active cross-sectional area of 4 cm^2. The single cell polarization curves were collected after the operation condition of single cell has been stable for half an hour. The DMFC was operated as the following conditions: 1.0 M CH_3OH, 1.0 ml/min, 90 °C, 0.2 MPa oxygen pressure.

3. Results and discussion

The chemical compositions of these Pt–Fe/C catalysts determined by EDX are shown in Table 1. The Pt metal loading in all the Pt–Fe/C catalysts are similar (from 18.2 to 19.9 wt.%). However, the Pt–Fe/C prepared from EG method has the Pt–Fe ratio of 93:7, which is smaller than that of Pt–Fe/C catalysts prepared by the two-step method (79:21). This may be attributed to the modified polyol synthesis method, in which Fe could not be reduced completely under the adopted experimental conditions. XRD patterns for these prepared Pt-based catalysts are shown in Fig. 1a. The peak of 25°, which is the wide graphite (0 0 2) peak, suggests that XC-72 carbon black support has a good graphite characteristic. No Fe^0 or Fe_2O_3 peaks are observed in the XRD patterns of all these Pt–Fe/C samples, this is probably because their phases were not fully developed or their particle sizes were relatively small for in-house Pt–Fe/C and moderated treated Pt–Fe/C300 sample, and because iron were involved in the formation of alloy for Pt–Fe/C900B. With the temperature increasing, the diffraction peaks of Pt become sharp, which indicates an aggregation of Pt particles. Because the Pt (2 2 0) peak is isolated from the diffraction peaks of the carbon black support, the mean Pt particle sizes for all these catalysts were calculated from Scherrer's formula based on Pt (2 2 0) [28], shown in Fig. 1b.

$$L = \frac{0.9\lambda_{K\alpha 1}}{B_{(2\theta)} \cos\theta_{max}} \quad (3)$$

where L is the mean size of Pt particle, $\lambda_{K\alpha 1}$ is the wavelength of X-ray (Cu Kα, $\lambda_{K\alpha 1}$ = 1.5418 Å), θ_{max} is the maximum angle of Pt (2 2 0) peak and the $B_{(2\theta)}$ is half peak broadening for Pt (2 2 0) in radians. Lattice parameters of these Pt-based catalysts can be evaluated from the angular position of Pt (2 2 0) peak maxima [28]. Table 1 summarizes the XRD results. The mean Pt particle size of Pt/C and Pt–Fe/C are very small, 2.4 and 2.2 nm, respectively. Pt particle size is slightly smaller when Fe was added. This result is not consistent with Toshima's work [19], they prepared poly(*N*-vinyl-2-pyrrolidone) protected Cu/Pd (1:1) alloy

Table 1
Chemical compositions of prepared Pt–Fe/C catalysts as determined by EDX

Catalysts sample	Catalysts compositions	Pt loading (wt.%)	Catalysts compositions (Pt:Fe)
1	20 wt.% Pt/C	19.9	–[a]
2	20 wt.% Pt–Fe/C300	19.0	93:7
3	20 wt.% Pt–Fe/C900B	18.2	79:21
4	20 wt.% Pt–Fe/C300 (after a 40-h-test)	19.2	95:5

[a] Not paragraphed.

clusters, whose particle size is larger than that of Pt cluster. In our work, the mean particle size of Pt–Fe/C decreases with the Fe content increasing in a wide range of Pt–Fe ratio. This may be attributed to no use of protective agent and different detailed synthesis conditions. Pt–Fe/C300 catalyst has a mean particle size of 2.8 nm, which is smaller than that of Pt–Fe/C900 (4.4 nm). Pt–Fe/C-900HB has the largest Pt particle size (6.2 nm) among these samples. This suggests that the Pt particle does not grow much larger after hydrogen treatment at moderated temperature (300 °C) and grow larger after high temperature (900 °C) treatment. Pt–Fe/C900 prepared by EG method has a smaller particle size than that of catalyst prepared by the two-step method, which suggests the EG method can efficiently decrease Pt particle size. Lattice parameters are 3.912, 3.908 and 3.892 Å for Pt–Fe/C300, Pt–Fe/C900 and Pt–Fe/C900B samples, respectively. The lattice parameter was found to be 3.924 Å for pure platinum and 3.865 Å for Pt_3Fe alloy [29]. This means that Pt–Fe/C has partly alloyed after 300 °C-reduced treatment, even under higher temperature, and the Pt–Fe alloy could not form further, the Pt–Fe/C900B sample is the most Pt–Fe alloy catalyst. Therefore it could be logically concluded that more Fe content and high temperature treatment are the two key factors in forming a better Pt–Fe alloy catalyst.

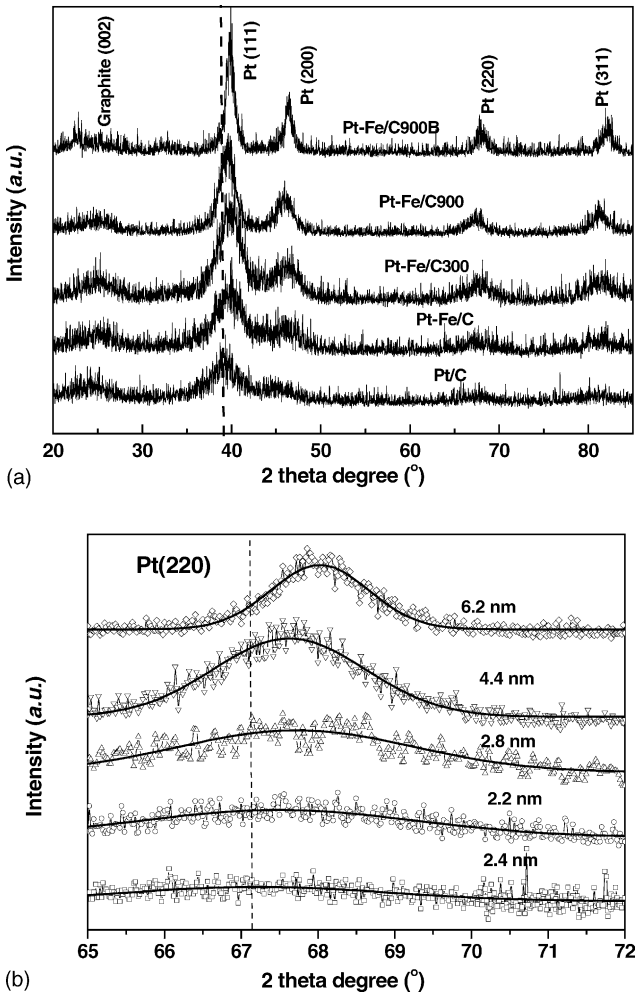

Fig. 1. (a) Powder XRD patterns of the Pt-based catalysts. (b) Powder XRD patterns of prepared the Pt-based catalysts: detailed Pt (2 2 0) peaks.

Fig. 2 is the TEM image of Pt–Fe/C300 and histograms of these Pt-based catalysts. The histogram of Pt particle size of Pt/C based on measuring over 300 Pt particles shows that the Pt particle size has a relatively narrow particle size dispersion of 1–5 nm, the mean particle size is 2.9 nm, which is of fairly consistence with the XRD measurements. In comparison, the Pt particle size in Pt–Fe/C300 increase and the particle size distribution becomes wider, from 1 to 9 nm, more than 82% Pt particles are between 2 and 5 nm, centered at 3.4 nm, which is also in agreement with XRD measurements. The Pt–Fe/C900 catalyst has a particle size distribution of 2–11 nm and the mean particle size is 5.1 nm, which is larger than Pt/C or Pt–Fe/C catalyst under moderated temperature treatment. In contrast, the particle size distribution of Pt–Fe/C900B catalyst is very wide, from 3 to 18 nm with mean particle size of 7.3 nm, big Pt particles with size of 18 nm are observed in Pt–Fe/C900B catalyst occasionally, this suggests that the Pt–Fe/C900B, prepared by two-step preparation method, has a wide Pt particle distribution than that of Pt–Fe/C900 prepared by EG method.

Cyclicvoltammetry tests (CV) were performed in 1.0 M $HClO_4$ (as shown in Fig. 3). From the hydrogen adsorptions peak areas in the CV curves and the Pt single crystallite hydrogen adsorptions constant 210 $\mu C/cm^2$ Pt, the electrochemical surface areas for these catalysts can be calculated, shown in Table 2. The chemical surface area of these Pt-based catalysts can also be calculated using the following equation:

$$S_{CSA} = \frac{6 \times 10^4}{\rho d} \quad (4)$$

where d is the mean Pt particle in Å (from TEM results) and ρ is the density of Pt metal (21.4 g/cm^2). Then the Pt

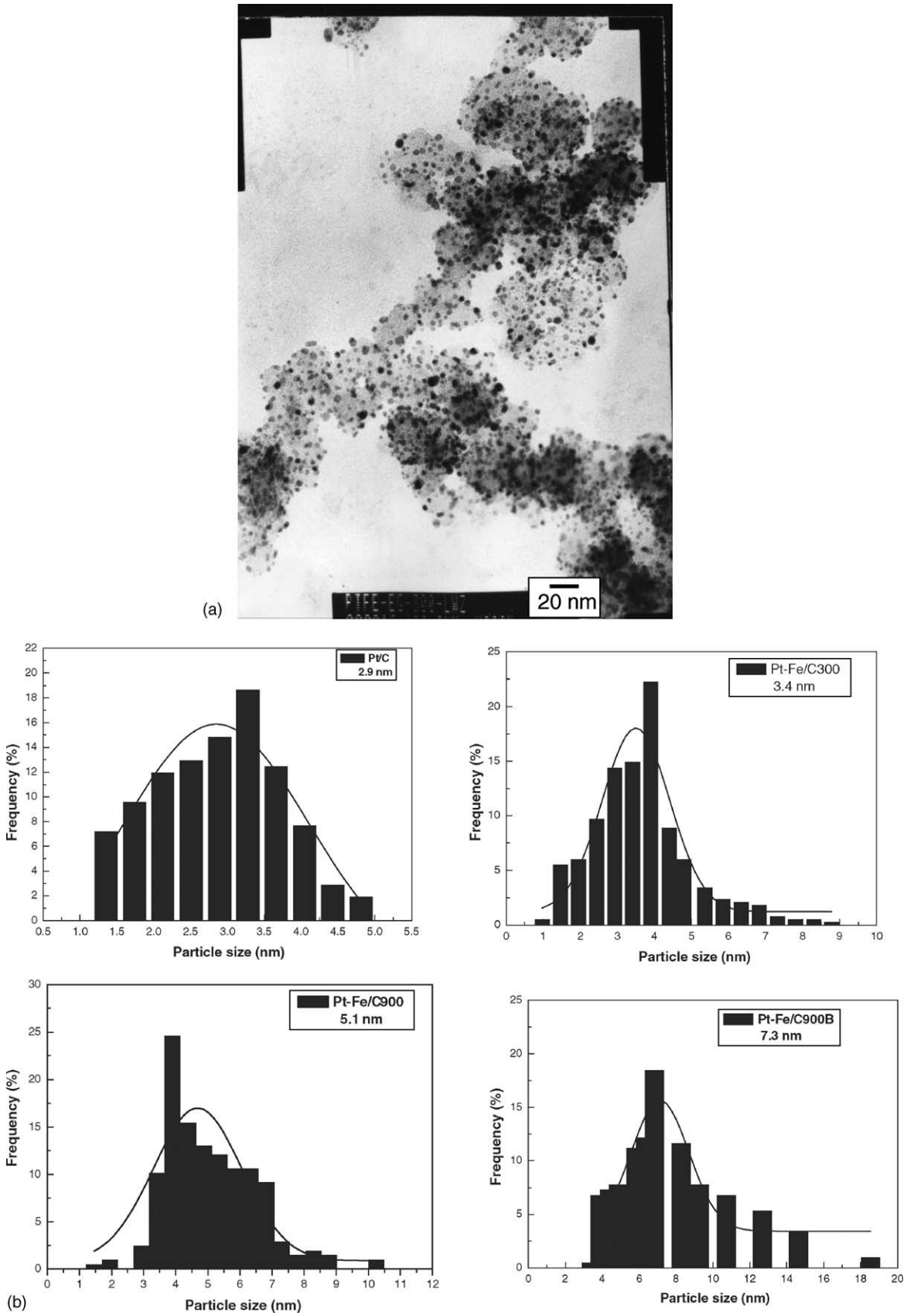

Fig. 2. (a) TEM image of Pt–Fe/C300 catalyst (250 K). (b) Histograms of Pt/C, Pt–Fe/C300, Pt–Fe/C900 and Pt–Fe/C900B catalysts.

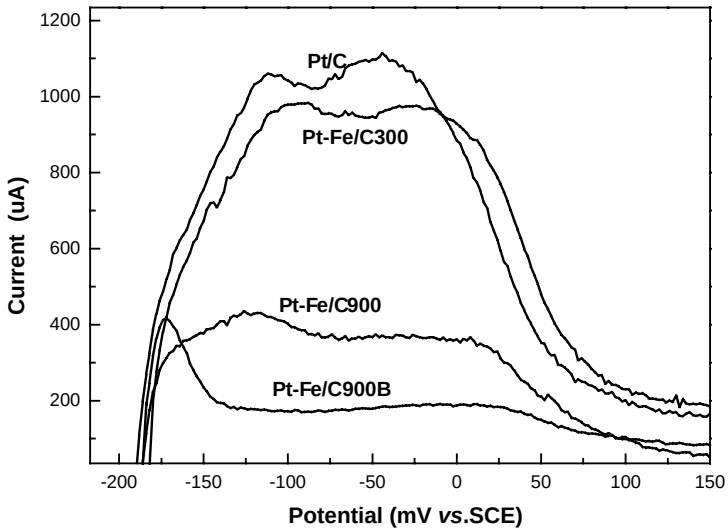

Fig. 3. Cyclicvoltammetry curves of prepared Pt-based catalysts 1.0 M $HClO_4$, recorded at 50 mV/s.

utilization efficiency for RDE can be calculated:

$$\text{Pt utilization efficiency} = \frac{S_{\text{ECSA}}}{S_{\text{CSA}}}$$

Pt–Fe/C300 has an electrochemical surface area of 63.6 m^2/g, slightly lower than that of Pt/C catalyst (68.3 m^2/g), the Pt utilization efficiencies for the two catalysts are about 76 and 72%, which is in good agreement with other's work [16]. However, the Pt utilization efficiencies of Pt–Fe/C900 and Pt–Fe/C900B are only about 54 and 40%, respectively. The Fe enrichment on the surface due to high temperature treatment lowering the surface area of Pt may be responsible for the lower utilization of Pt in liquid electrolyte.

Rotating disk electrode (RDE) tests were conducted in 1.0 $HClO_4$, which is a week anion-adsorption acid and can be used to evaluate the mass activity well [32]. There are two ways to express the activity of Pt based catalysts. One is mass activity (MA), which is the current per amount of catalyst, and the other is specific activity (SA), which is for surface area of catalyst. The MA has practical meaning for fuel cells, because the cost of electrode is largely depend on the total catalysts, while the SA provides catalytic information of Pt atoms in the surface. The MA and SA for these Pt-based catalysts at potential of 660 mV (SCE = 0.9V·RHE) were obtained through formulas (1) and (2). The ORR current is negative, in order to evaluate the activity of these Pt–Fe/C catalysts, the absolute value of ORR for these Pt–Fe/C catalysts are used. From Fig. 4, It is found that Pt–Fe/C300 has the highest MA of 21.5 mA/mg Pt and the highest SA of 341 mA/m^2 Pt, which is higher than that of Pt/C, Pt–Fe/C900 and Pt–Fe/C900B catalysts. Pt–Fe/C900B has the second largest specific activity of 288 mA/m^2 Pt, which may be attributed to its best Pt–Fe alloy characteristic, but the mass activity of Pt–Fe/C900B is only 4.1 mA/mg Pt, which is the lowest among these Pt-based catalysts (as shown in Table 3). This is mainly attributed to Pt particle agglomeration due to high temperature treatment and the Pt metal specific area decreased sharply. Watanabe and coworkers [31–34] used sputtering technique to prepare Pt–Fe alloy and CV, XPS, STM, EQCM showed that Fe dissolved out rapidly together with Pt at the immersion and the following potential cycles (CV, 0.05–1.0 V), but Pt re-deposited immediately after dissolution on the surface, resulting a stable and well-ordered (1 1 1)-oriented Pt surface layer (ca. 0.1 nm XPS characterization). In our case, the Fe could also dissolve from Pt–Fe/C catalysts and the enhanced ORR for these Pt–Fe/C catalysts were found in RDE tests.

Table 2
Characterization of prepared Pt–Fe/C catalysts by XRD and TEM

Catalyst	XRD Particle size (nm)	Lattice parameter (Å)	TEM Particle size (nm)
Pt/C	2.4	3.927	2.9
Pt–Fe/C	2.2	3.921	–[a]
Pt–Fe/C300	2.8	3.912	3.4
Pt–Fe/C900	4.4	3.908	5.1
Pt–Fe/C900B	6.2	3.892	7.3

[a] Not paragraphed.

CV and RDE experiments are also used to test the methanol tolerant properties of these Pt–Fe/C catalysts in a 1.0 M $HClO_4$+0.1 M CH_3OH electrolyte. In Fig. 5, although the initiate methanol oxidation voltages for the two catalysts do not shift, the hydrogen desorption peak for Pt–Fe/C300 is higher than that of the Pt/C sample while the methanol oxidation peak for Pt–Fe/C300 is smaller than that of Pt/C catalyst, this is due to the smaller electrochemical surface area and less methanol oxidation activity for Pt–Fe/C300 than that for Pt/C. RDE test results are shown in Fig. 6, in 1.0 M $HClO_4$ + 0.1 M MeOH electrolyte, the potential reaches ca. 650 or 617 mV (SCE), MeOH begin oxidizing at Pt/C and Pt–Fe/C300 catalysts, at ca. 515 or 458 mV (SCE),

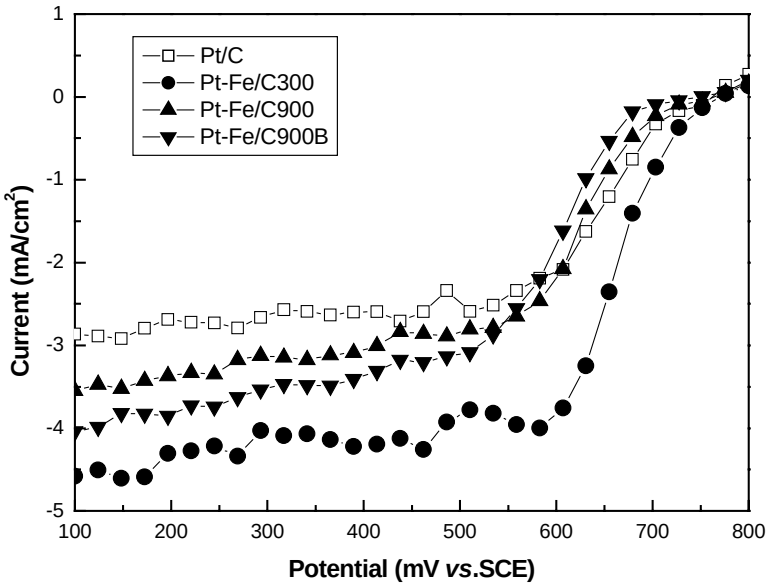

Fig. 4. RDE cathodic curves for prepared Pt-based catalysts in 1.0 M $HClO_4$ at 2500 rpm, recorded at 5 mV/s.

the methanol oxidizing peak reach maximum points. The reduction of O_2 as catalyzed by the Pt/C and Pt–Fe/C300 catalysts then commence, producing slightly rising currents. With the scan potential decreasing to ca. 300 mV, the currents rise to yield a flat plateau, which lower about 300 mV than that obtained in $HClO_4$ electrolytic solution without methanol. This means that the addition of MeOH dramatically reduces the limited current of RDE and the limited current decreased with the increasing methanol concentration. The RDE performance of Pt–Fe/C300 is similar as that Pt/C catalyst. Our experimental results are not of consistence with the Pt–Ni alloy, which exhibits 11 times higher limiting current density as comparing to Pt in RDE tests in 1 M H_2SO_4/0.5 M CH_3OH [30]. Maillard et al. [35] compared the ORR for Pt–Cr/C (Pt:Cr 1:1, 10 wt.%) and Pt/C (40 wt.%) with the similar particle size using RDE technique in a methanol containing perchloric electrolyte (0.1 M $HClO_4$ + 0.1 M CH_3OH) and found that Pt–Cr/C is more active catalyst than Pt/C for ORR. However, in our case, the methanol oxidation peaks for both catalysts are obvious, nearly no methanol oxidizing peak shift between these two catalysts and the limiting current densities are almost same, this suggests that the similar mechanism of ORR under methanol oxidation competition for Pt/C and Pt–Fe/C300 catalysts, this is probably due to the less Fe content in our sample and different preparation methods (Table 3).

The DMFC polarization curves for these Pt-based cathode catalysts are tested and shown in Fig. 7 and summarized in

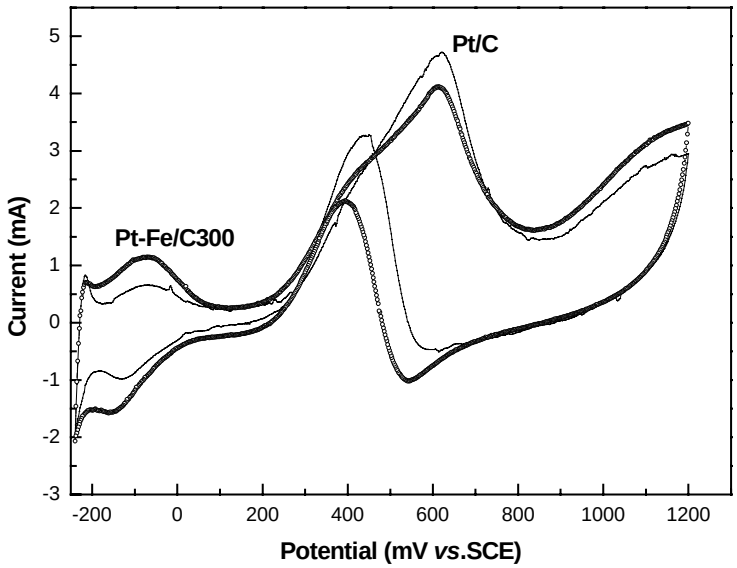

Fig. 5. Cyclicvoltammetry curves of Pt/C and Pt–Fe/C300 catalysts in 1.0 M $HClO_4$ + 0.1 M MeOH, recorded at 50 mV/s.

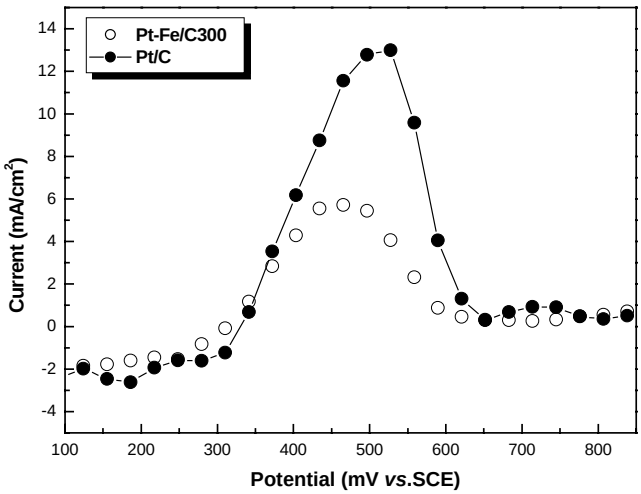

Fig. 6. RDE cathodic curves of Pt/C and Pt–Fe/C300 catalysts in 1.0 M $HClO_4$ + 0.1 M MeOH at 2500 rpm, recorded at 5 mV/s.

Table 3
Electrochemical characterizations for the prepared Pt–Fe/C catalysts by CV and RDE

Catalysts	Electrochemical surface area (m^2/g)	Pt utilization efficiency (%)	At 660 mV (vs·SCE)	
			Mass activity (mA/mg Pt)	Specific activity (mA/m^2 Pt)
Pt/C	68.3	72	9.3	137
Pt–Fe/C300	63.6	76	21.5	341
Pt–Fe/C900	30.4	54	5.4	176
Pt–Fe/C900B	14.3	40	4.1	288

Table 4. Based on particle size and Pt surface species consideration, Pt/C300 (Pt/C reduced in H_2/Ar at 300 °C for 2 h) was also employed as cathode catalyst in DMFC test. From the Fig. 7, Pt–Fe/C300 catalyst shows an enhanced ORR activity and better performance in both activity controlled region and high current density region than other Pt-based catalysts, i.e. the OCV (open circuit voltage) of the single cell with Pt–Fe/C300 is 0.694 V, which is 11 mV higher than that of Pt/C catalyst. At 0.650 V the current density for the cell with Pt–Fe/C300 is 6.3 mA/mg Pt, while that of cell with Pt/C is only 1.8 mA/mg Pt, this is consistence with RDE results, which strongly support the increase of performance in single cell originated from enhancement of ORR for Pt–Fe/C300 catalyst. Pt–Fe/C900 exhibits lower ORR activity and performance and Pt–Fe/C900B shows comparatively higher performance than that of Pt/C catalyst, this is because that Pt–Fe/C900B has a better Pt–Fe alloy form. The power density of single cell with Pt–Fe/C300 can reach 118 mW/cm^2, while that of single cell with Pt/C catalyst is only 92 mW/cm^2.

About the enhancement in ORR activity of Pt-based alloy catalysts, many research works are reported. Jalan and Taylor studied the ORR at Pt alloys supported on carbon black in phosphoric acid fuel cells (PAFC) and claimed that the enhancement of Pt catalytic activity for the reaction results from the shortening of Pt–Pt interatomic distances by alloying [36]. Appleby et al demonstrated a volcano type behavior in the relationship between the electrocatalytic activity and the adsorbate bond length [37]. It is shown that the lattice contractions due to alloying resulted in a more favorable Pt–Pt distance for the dissociative adsorption of O_2, while maintaining the favorable electronic property of Pt. This view of favorable Pt–Pt distances was supported by Mukerjee and Srinivasan, they found no electronic structure change [38], on basis of the results with XRD and XPS at supported Pt binary alloys in PEFCs. Further, they [39]

Table 4
Summary of performances of direct methanol single cells adopting prepared Pt/C or Pt–Fe/C as cathodic catalysts

Catalysts	Open circuit voltage (V)	Current density (mA/cm^2)					Maximum power density (mW/cm^2)
		0.65 V	0.6 V	0.5 V	0.4 V	0.3 V	
Pt/C	0.683	1.8	9.8	65	158	298	92
Pt/C300	0.681	1.5	7.5	70	197	319	98
Pt–Fe/C300	0.694	6.3	22.0	108	250	382	118
Pt–Fe/C900	0.661	1.1	8.1	65	167	273	82
Pt–Fe/C900B	0.678	2.4	16.0	85	215	354	112

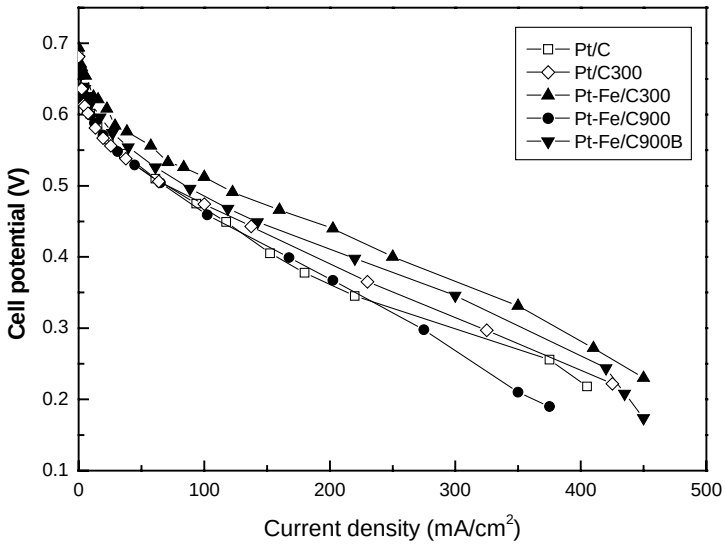

Fig. 7. Comparison of single cell polarization curves for the DMFC in presence of Pt/C, Pt–Fe/C300, Pt–Fe/C900, Pt–Fe/C900B cathode catalysts (1.0 mg Pt/cm^2); anode: Pt–Ru/C (20 wt.% Pt, 10 wt.% Ru, Johnson Matthey Corp.; catalyst loading: 2.0 mg Pt–Ru/cm^2); electrolyte membrane: Nafion-115® (DuPont) membranes; operation temperature: 90 °C; methanol concentration: 1.0 M CH_3OH; flow rate: 1.0 ml/min, oxygen pressure: 0.2 MPa.

rationalized the enhanced electrocatalysis later with in situ XANES and EXAFS on the basis of the interplay between the electronic (Pt d-vacancy) and geometric the factors (Pt coordination number) on the one hand, and their effect on the chemisorption behavior of OH species from the electrolyte. However, Glass et al. [40] found no activity enhancement for the ORR on bulk Pt–Cr alloys in hot H_3PO_4 and suggested the possibility of differences in electrochemical properties of bulk versus supported fine particles. On the other hand, Paffett et al. [41] attributed higher activities for the ORR on bulk Pt–Cr alloys in H_3PO_4 to surface roughening, and hence increased Pt surface area, caused by the dissolution of the non-precious metal Cr. Although this view cannot explain the enhancement of the initial ORR activity of Pt–Cr alloy. A study on supported Pt–Co alloys in hot H_3PO_4 by Beard and Ross revealed the possibility that particle termination, particularly at the '100' vicinal planes in the catalysts, is the reason for the enhanced electrocatalysis [42]. However, a study on the catalytic activity and stability of supported Pt–Co alloys with well-defined structures by Watanabe et al. [43] demonstrated that both Co and Pt dissolve out preferentially from small-size alloy particles and Pt re-deposits on the surfaces of large-size ones in hot H_3PO_4. As for the result, the alloy with a disordered crystallite structure, which is more corrosion-resistant than an ordered one, maintains higher electrocatalytic activity for a longer time due to the active alloy surfaces with a relatively large surface area. Recently, Min et al. [44] used CV, X-ray absorption near-edge structure (XANES) and PEM single cell test and claimed the structure sensitivity of Pt and Pt-based alloy catalysts for oxygen reduction seems associated with the adsorption strength of oxygen intermediates on the Pt surface. The Pt-based alloy catalysts showed significantly higher specific activities than Pt-alone catalysts with the same surface area. The phenomenon comes from the reduced Pt–Pt neighboring distance, which is favorable for the adsorption of oxygen. Kim et al. [45,46] studied the surface and catalytic properties of Pt–Fe/C or Pt–Cr/C catalysts in PAFCs, they found enhancement in mass activity for ORR when acid-treated Pt–Fe/C or Pt–Cr/C catalysts were used and suggested an enrichment of Pt surface area due to the transitional metal leaching out.

In our study, it is interesting to note that the Pt–Fe/C300 has shown an enhanced ORR activity and better single cell performance than that of Pt/C and other Pt–Fe/C catalysts. The Pt–Fe/C300 catalyst consisted of most Pt and little Fe (Pt:Fe = 93:7) and was reduced at moderated temperature (300 °C). As we knew, more Pt^0 species exist after Pt–Fe/C catalyst reduced at 300 °C. This Pt^0 species are believed to be more active for ORR. However, Pt–Fe/C300 shows an enhanced ORR activity than that of Pt/C under identical reduction treatment (Pt/C300). This could be attributed to addition of Fe to Pt/C catalyst. The more electropositive based metal (Fe) to which the oxygen species is attached, provides an electrochemical force that favors the four-electron oxygen reduction electrochemical pathways, consequently improve the ORR activity of the catalyst [13,14]. For a Pt–Fe/C catalyst under moderate temperature treatment, another factor is not ought to be neglected. At this comparatively low treatment temperature, Fe cannot form Pt–Fe alloy completely and was more prone to corrode at the operation voltage at 90 °C, the Fe ion could promote the ORR activity. We confirmed this presupposition by using RDE test with adding some Fe ion in $HClO_4$ solution. As the Fig. 8 shown, the mass activity for Pt/C catalyst in 1.0 M $HClO_4$ + 100 ppm Fe^{3+} electrolyte is 13.4 mA/mg Pt at 660 mV (SCE), which is higher than that of Pt/C in 1.0 M $HClO_4$ (9.3 mA/mg Pt), however when the Fe^{3+} increases

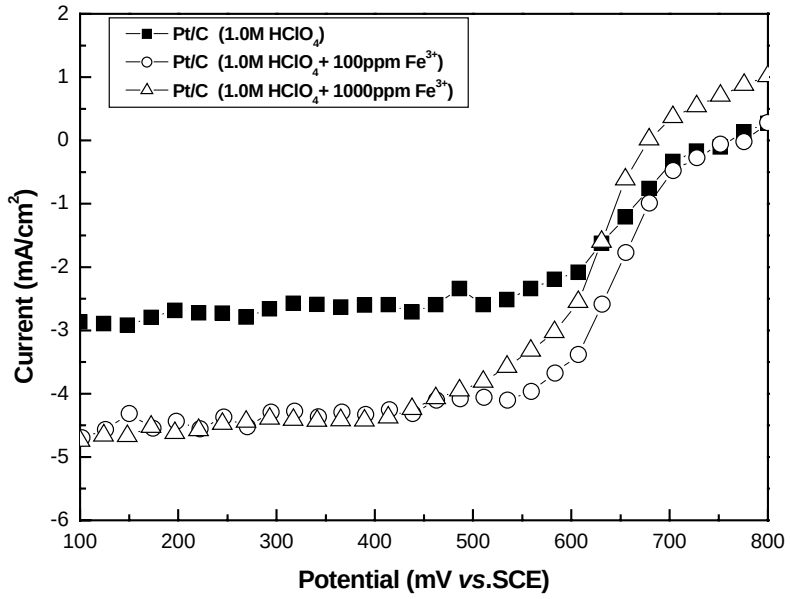

Fig. 8. RDE cathodic curves for Pt/C in 1.0 M $HClO_4$ at 2500 rpm without or with different Fe ion, recorded at 5 mV/s.

to 1000 ppm, the mass activity decreases to 2.8 mA/mg Pt, lower than that of Pt/C in 1.0 M $HClO_4$. It was also found that the limited currents for Pt/C catalyst increased considerably when 100 or 1000 ppm Fe ion was added in $HClO_4$ electrolyte. Sun accounts the Fe promotion effect on ORR activity for Pt/C to the higher H_2O_2 decomposition activity when Fe^{3+} and Pt/C are co-presented [47]. The ideal ORR is a four-electron transferring reaction (shown as reaction [5]), which only occurred when oxygen is dissociatively adsorbed on Pt-based catalysts. However, in most catalysts, including Pt/C catalysts, oxygen does not dissociate on Pt sites and then follows the [6] reaction, which will lower the open circuit voltage (OCV).

$$O_2 + 4H^+ + 4e^- \rightarrow 2H_2O, \quad E_0 = 1.23\,V \tag{5}$$

$$O_2 + 2H^+ + 2e^- \rightarrow 2H_2O_2, \quad E_0 = 0.68\,V \tag{6}$$

Fe^{2+} will be oxidized to Fe^{3+} when Fe^{2+} sissoluted in a oxygen saturated $HClO_4$ solution, Fe^{3+} could react with H_2O_2 to form the medium products as following fomula:

$$Fe^{3+} + H_2O_2 \rightarrow [Fe(III)\text{–}O_2H]^{2+} + H^+ \tag{7}$$

$$Fe^{3+} + H_2O_2 + H_2O \rightarrow [Fe(III)\text{–}(OH)(O_2H)]^+ + 2H^+ \tag{8}$$

$[Fe(III)\text{–}O_2H]^{2+}$ and $[Fe(III)\text{–}(OH)(O_2H)]^+$ could react with Fe^{3+} to product O_2 when Pt/C catalyst exists, this will promote the H_2O_2 to decompose to H_2O:

$$[Fe(III)\text{–}O_2H]^{2+} + Fe^{3+} \rightarrow 2Fe^{2+} + H^+ + O_2 \tag{9}$$

$$[Fe(III)\text{–}(OH)(O_2H)]^+ + Fe^{3+} \rightarrow 2Fe^{2+} + H_2O + O_2 \tag{10}$$

In our study, when Fe^{3+} increases to 1000 ppm, it is clear that current at 800 mV (SCE) is about 1.0 mA/cm^2, which means the Fe^{2+}/Fe^{3+} reaction potential cannot be ignored, the RDE cathodic curves includes ORR and Fe^{2+}/Fe^{3+} reactions, this positive Fe^{2+}/Fe^{3+} decrease the ORR negative current at 660 mV (SCE). EDX analysis shows that the Pt–Fe/C300 has a Pt:Fe ratio of 93:7, however, increasing to 95:5 after a 40-h DMFC test, which means near 30 at.% Fe content loss during the test. Therefore, in our study, the improvement in the performance of Pt–Fe/C for oxygen reduction may be partly due to the higher peroxide decomposition activity of Pt in presence of dissolved Fe when the operation was performed for a time. Further work is required on identification of the ORR enhancement mechanism and the optimum Fe content in Pt–Fe/C300 catalyst.

4. Conclusions

This paper presents a polyol synthesis strategy (EG method) to prepare Pt–Fe/C catalysts, then the heat-treatments under hydrogen atmosphere at 300 or 900 °C were employed. Pt–Fe/C alloy catalyst was prepared by a two-step method (wet-incipience method) as compared sample. XRD patterns and TEM images show that the particle size of Pt–Fe/C300 sample does not increase too much, with a mean particle size of 2.8 nm (XRD), 3.6 nm (TEM) and partly-formed Pt–Fe alloy was found in this sample. Pt–Fe/C900B catalyst has the biggest mean particle size (6.2 nm) and a wide particle size distribution (3–18 nm) although it has the best Pt–Fe alloy form. CV results show that Pt–Fe/C300 has larger electrochemical surface area than other Pt–Fe/C and the highest Pt utilization ratio of 76% among these Pt-based catalysts. RDE cathodic curve shows that Pt–Fe/C300 has the highest ORR mass activity and specific activity, while Pt–Fe/C900B has the second

highest ORR specific activity in a 1.0 M $HClO_4$, this can be attributed to an alloy effect. Pt–Fe/C300 catalyst does not appears to be a more active catalyst than Pt/C for ORR in methanol-containing perchloric acid electrolyte (1.0 M $HClO_4$ + 0.1 M MeOH). Further, Pt–Fe/C300 exhibits the higher ORR activity and better performance than other Pt/C or Pt–Fe/C catalysts in direct methanol single cell test, the increasing of cell performance may be attributed to more Pt^0 species existing and Fe ion corrosion from catalysts, which is believed to facilitate the H_2O_2 decomposition of Pt sites.

Acknowledgements

This work is partly supported by the National Natural Science Foundation of China (Grant Nos. 29976006 and 20173060) and the Innovation Foundation of Dalian Institute of Chemical Physics.

References

[1] A. Hamnett, Catal. Today 38 (1997) 445.
[2] B.D. McNicol, D.A.J. Rand, K.R. Williams, J. Power Sources 83 (1999) 15.
[3] S. Wasmus, A. Küver, J. Electroananl. Chem. 461 (1999) 14.
[4] A.S. Arico, S. Srinivasan, V. Antonucci, Fuel Cells 2 (2001) 1.
[5] X.M. Ren, P. Zelenay, A. Thomas, J. Javey, S. Gottesfeld, J. Power Sources 86 (2000) 111.
[6] Fuel Cell Handbook, fifth ed., EG&G Services Parsons, Inc., 2000.
[7] V. Trapp, P.A. Christensen, A. Hamnett, J. Chem. Soc., Faraday Trans. 21 (1996) 4311.
[8] R.W. Reeve, P.A. Christensen, A. Hamnett, S.A. Haydock, S.A. Roy, J. Electrochem. Soc. 145 (1998) 3463.
[9] H. Tributsch, M. Bron, M. Hilgendorff, H. Schulenburg, I. Dorbant, V. Eyert, P. Bogdanoff, S. Fiechter, J. Appl. Electrochem. 31 (2001) 739.
[10] E. Antolini, Mater. Chem. Phys. 78 (2003) 563.
[11] A.K. Shukla, M. Neergat, B. Parthasarathi, V. Jayaram, M.S. Hegde, J. Electroanal. Chem. 504 (2001) 111.
[12] S. Mukerjee, S. Srinivasan, M.P. Soriaga, J. McBreen, J. Electrochem. Soc. 142 (1995) 1409.
[13] A.S. Arico, A.K. Shukla, H. Kim, S. Park, M. Min, V. Antonucci, Appl. Surf. Sci. 172 (2001) 33.
[14] M. Neergat, A.K. Shukla, K.S. Gandhi, J. Appl. Electrochem. 31 (2001) 373.
[15] P. Stoneheart, J. Appl. Electrochem. 22 (1992) 995.
[16] S. Mukerjee, J. Appl. Electrochem. 20 (1990) 537.
[17] T. Maoka, T. Kitai, N. Segawa, M. Ueno, J. Appl. Electrochem. 26 (1996) 1267.
[18] Y.Wang.J.W. Ren, K. Deng, L.L. Gui, Y.Q. Tang, Chem. Mater. 12 (2000) 1622.
[19] N. Toshima, Y. Wang, Langmuir 10 (1994) 4574.
[20] X.P. Yan, H.F. Liu, Y. Liew, J. Mater. Chem. 6 (2001) 3387.
[21] Z.H. Zhou, S.L. Wang, W.J. Zhou, G.X. Wang, L.H. Jiang, W.Z. Li, S.Q. Song, J.Q. Liu, G.Q. Sun, Q. Xin, Chem. Commun. 1 (2003) 394.
[22] W.J. Zhou, Z.H. Zhou, S.Q. Song, W.Z. Li, P. Tsiakaras, G.Q. Sun, Q. Xin, Appl. Catal. B, 2003, 273.
[23] W.Z. Li, C.H. Liang, J.S. Qiu, W.J. Zhou, H.M. Han, Z.B. Wei, G.Q. Sun, Q. Xin, Carbon 40 (2002) 791.
[24] W.Z. Li, C.H. Liang, W.J. Zhou, J.S. Qiu, Z.H. Zhou, G.Q. Sun, Q. Xin, J. Phys. Chem. 107 (2003) 6292.
[25] Askoylu, A.E., Madalena, M., Freitas; Figueiredo, J.L. Appl. Catal. A 192 (2000) 29.
[26] G. Tamizhmani, J.P. Dodelet, D. Guay, J. Electrochem. Soc. 143 (1996) 18.
[27] Z.B. Wei, S.L. Wang, B.L. Yi, J.G. Liu, L.K. Chen, W.J. Zhou, W.Z. Li, Q. Xin, J. Power Sources 106 (1999) 364.
[28] V. Radmilovic, H.A. Gasteiger, P.N. Ross Jr., J. Catal. 154 (1995) 98.
[29] W.F. McClune, Power Diffraction File, International Center for Diffraction Data, Pennsylvania, USA, 1981.
[30] T.J. Schmidt, U.A. Paulus, H. A Gasteiger, R.J. Behm, J. Electroanal. Chem. 508 (2001) 41.
[31] T. Toda, H. Igarashi, H. Uchida, M. Watanabe, J. Electrochem. Soc. 146 (1999) 3750.
[32] T. Toda, H. Igarashi, M. Watanabe, J. Electroanal. Chem. 460 (1999) 258.
[33] L. Wan, T. Moriyama, M. Ito, H. Uchida, M. Watanabe, Chem. Commun. (2002) 58.
[34] H. Uchida, H. Ozuka, M. Watanabe, Electrochim. Acta 47 (2002) 3629.
[35] F. Maillard, M. Martin, F. Gloaguen, J.-M. Léger, Electrochim. Acta 47 (2002) 3431.
[36] V.M. Jalan, E.J. Taylor, J. Electrochem. Soc. 130 (1983) 2299.
[37] J. Appleby, Energy 11 (1986) 13.
[38] S. Mukerjee, S.J. Srinivasan, J. Electroanal. Chem. 357 (1993) 201.
[39] S. Mukerjee, S. Srinivasan, M.P. Soriage, J. Phys. Chem. 99 (1995) 4577.
[40] J.Y. Glass, G.L. Gahen Jr., G.E. Stoner, E.T. Taylor, J. Electrochem. Soc. 134 (1987) 58.
[41] M.T. Paffett, J.G. Beery, S. Gottesfeld, J. Electrochem. Soc. 135 (1988) 1431.
[42] B.C. Beard, P.N. Ross, J. Electrochem. Soc. 137 (1990) 3368.
[43] M. Wantanabe, K. Tsurumi, T. Mizukami, T. Nakamura, P. Stonehart, J. Electrochem. Soc. 141 (1994) 2659.
[44] M.K. Min, J. Cho, K.W. Cho, H. Kim, Electrochim. Acta 45 (2000) 4211.
[45] K.T. Kim, J.T. Hwang, Y.G. Kim, J.S. Chung, J. Electrochem. Soc. 140 (1994) 31.
[46] T. Kim, Y.G. Kim, J.S. Chung, J. Electrochem. Soc. 142 (1995) 1531.
[47] Z. Sun, A.C. Tseung, Electrochem. Solid State Lett. 3 (2000) 413.